References

1. J. Ellis, G. M. Mockler, and E. Sinn, *Inorg. Chem.*, **20**, 1206 (1981).
2. H. A. Kuska, M. F. Farona, P. Pappas, and S. Potterton, *J. Coord. Chem.*, **1**, 259 (1971).
3. F. M. Ashwamy, C. A. Mcauliffe, R. V. Parish, and J. Tames, *J. Chem. Soc. Dalton Trans.*, **1391** (1985).
4. D. Benson, "Mechanisms of Oxidation by Metal Ions", Elsevier, N.Y., 1976.
5. P. S. Dixit and K. Srinivasan, *Inorg. Chem.*, **27**, 4507 (1988).
6. K. Srinivasan, P. Michaud, and J. K. Kochi, *J. Am. Chem. Soc.*, **108**, 2309 (1986).
7. J. T. Groves, W. J. Kruper, and R. C. Haushalter, *J. Am. Chem. Soc.*, **108**, 6375 (1980).
8. C. L. Hill and R. B. Brown, *J. Am. Chem. Soc.*, **108**, 536 (1986).
9. J. T. Groves and M. K. Stern, *J. Am. Chem. Soc.*, **109**, 3812 (1987).
10. H. E. Fonouni, S. Krishnan, D. G. Kuhn, and G. A. Hamilton, *J. Am. Chem. Soc.*, **105**, 7672 (1983).
11. L. S. S. Reamonn, W. I. O'Sullivan, *J. Chem. Soc. Chem. Commun.*, 1012 (1976).
12. E. Guilmet and B. Meunier, *Tetrahedron Lett.*, **21**, 4449 (1980).
13. C. Eskenazi, G. Balavoine, F. Meunier, and H. Riviere, *J. Chem. Soc. Chem. Commun.*, 1111 (1985).
14. G. Cros and J. P. Costes, *C. R. Acad. Sc. Paris*, **294-II**, 173 (1982).
15. J. T. Groves and R. Quim, *J. Am. Chem. Soc.*, **107**, 5790 (1985).

Syntheses, X-ray Structures and Second Harmonic Generation Efficiencies of MAP (Methyl (2,4-dinitrophenyl)-aminopropanoate) Analogues

Joo-Hee Lee and Kimoon Kim*

Department of Chemistry and Center for Biofunctional Molecules, Pohang Institute of Science and Technology and Chemistry Group, Research Institute of Industrial Science and Technology, Pohang 790-784

Jong-Hyun Kim and Jong-Jean Kim

Department of Physics, Korea Advanced Institute of Science and Technology, Taejon 305-701

Received January 3, 1992

An attempt to improve the second harmonic generation (SHG) efficiency of MAP (methyl (2,4-dinitrophenyl)aminopropanoate) by modifying the substituents on the amino group of MAP is described. Several MAP analogues have been prepared using optically active amino acids alanine, phenylalanine and serine, and their SHG efficiencies measured. None of the MAP analogues exhibited SHG efficiencies as high as that of MAP. X-ray crystal structures of three MAP analogues have been determined. In the crystal structures of two of them, which were the derivatives of phenylalanine, two crystallographically-independent molecules existing in the asymmetric unit are aligned almost antiparallel. These structures are consistent with the very low SHG efficiencies of these compounds. On the other hand, the crystal structure of a serine derivative reveals substantial alignment of the dinitroaniline chromophore along the polar axis. However, the angle of 86.2° between the molecular charge tranfer axis and the polar axis of the crystal is still far away from the optimum value of 54.74° for the phase-matchable SHG. The structure is consistent with the SHG efficiency of this compound which is much higher than those of the phenylalanine derivatives but still lower than that of MAP. This study demonstrates the importance of the orientation of molecules in the crystal lattice in determining secod-order nonlinear optical properties of crystalline materials.

Introduction

There has been much interest in organic compounds with large second-order nonlinear optical (NLO) properties.[1-6] These materials can be used in second harmonic generation (SHG; i.e. doubling the frequency of laser light) or in electro-optic phase modulation. Effective SHG material have both high second-order molecular hyperpolarizability, β, and high second-order bulk susceptibility, $\chi^{(2)}$. Conjugated organic molecules with electron donating and electron accepting groups can exhibit large β.[2] However, if the molecular hyperpolarizability is to result in a nonzero macroscopic nonlinearity ($\chi^{(2)}$), the molecule must crystallize in a noncentrosymmetric space group. Unfortunately, many compounds with

large βs crystallize in centrosymmetric space groups, leading to materials with vanishing $\chi^{(2)}$.[7] Serveral methods to overcome this obstacle have been used including the introduction of chiral moieties[8] and/or functional groups that encourage asymmetric intermolecular hydrogen bonds,[9] and the variation of counter ion with ionic chromophore.[10]

Methyl (2,4-dinitrophenyl)aminopropanoate (MAP) (see below Figure 2) is one of the successful organic SHG materials.[8] MAP is a derivative of 2,4-dinitroaniline in which the amino group has been replaced by the methyl ester of the optically active amino acid alanine, which guarantees a noncentrosymmetric crystal structure. MAP is phase-matchable over its entire transparency range between 0.5 and 2.0 μm and has an NLO efficiency of 15 times that of $LiNbO_3$.[8] MAP crystallizes in the monoclinic space group $P2_1$ with two molecules per unit cell which are related by a twofold symmetry axis.[11] According to the theoretical analysis of Oudar and Zyss[12] the large optical nonlinearity of MAP is due primarily to the intramolecular charge transfer from the amino group to the *para*-nitro group rather than the *ortho*-nitro group. The orientation of the molecular *z* axis passing through the amino and *para*-nitro groups is approximately 79° from the unique axis of the crystal. Since a tilt of the molecular *z* axis from the unique crystal axis of 54.74° would be optimum for phase-matched SHG,[13] a higher NLO efficiency[14] could be obtained for the same chromophore with the optimum orientation of the molecule in the unit cell. We therefore decided to synthesize several MAP analogues having slightly different substituents on the amino group, hoping that such a modification on the molecular structure results in a better orientation of the molecule in the crystal and, in turn, a higher SHG efficiency. Here we present the results of such an attempt: syntheses, X-ray structures and SHG efficiencies of MAP analogues.

Experimental

All reagents were reagent grade and used without further purification. UV-Visible, IR and NMR spectra were recorded on a Hewlett-Packard 8452A UV-visible spectrophotometer, a Perkin-Elmer 843 IR spectrophotometer, and a Brucker AM-300 MHz NMR spectrometer, respectively. Mass spectra were obtained with a Kratos MS25RFA GC-Mass spectrometer. Elemental analyses were performed by Korea Basic Science Center.

2-(2,4-dinitophenylamino)propanoic acid (1). To a solution of L-alanine (0.536 g, 6.0 mmol) in 10 m*l* saturated sodium bicarbonate solution was added 2,4-dinitrofluorobenzene (DNFB) (0.5 m*l*, 4.0 mmol). After 3 h of stirring excess DNFB was removed by extraction with diethyl ether. Concentrated HCl was added to the aqueous phase until the pH of the solution became 2. The solid product was filtered and recrystallized from methanol (0.496 g, 32%). Anal. Calc. for $C_9H_9N_3O_6$: C, 42.35; H, 3.56; N, 16.47. Found: C, 42.03; H, 3.28; N, 16.29. Mass Spectrum (EI): m/z=255. ^{1}H-NMR ($CDCl_3$+DMSO-d_6) δ1.57 (3H, d), 4.27 (1H, m), 6.81 (1H, d), 8.19 (1H, dd), 8.92 (1H, d), 9.06 (1H, t).

Methyl-2-(2,4-dinitrophenylamino)propanoate (MAP) (2). To a solution of 1 (0.5 g) in 10 m*l* of methanol was added 0.4 m*l* of concentrated sulfuric acid. After 3 h of reflux the solution was cooled down to room temperature. When the pH of the solution was adjusted to 8-9 by adding sodium bicarbonate solution an oily product precipitated. The product was isolated by decantation and washed with water. Upon adding ethanol the oily product became a solid which was filtered and recrystallized from methanol (yield, ~85%). Anal. Calc. for $C_{10}H_{11}N_3O_6$: C, 44.61; H, 4.13; N, 15.61. Found: C, 44.50; H, 3.80; N, 15.36. Mass Spectrum (EI): m/z=269. ^{1}H-NMR ($CDCl_3$) δ1.59 (3H, d), 3.76 (3H, s), 4.34 (1H, m), 6.73 (1H, d), 8.22 (1H, dd), 8.84 (1H, d), 9.10 (1H, d).

2-(2,4-dinitophenylamino)-3-phenylpropanoic acid (3). This was prepared from L-phenylalanine (0.504 g, 3.0 mmol) and DNFB (0.5 m*l*, 4.0 mmol) by the same method as in **1**. Yield: 0.623 g, 62%. Anal. Calc. for $C_{15}H_{13}N_3O_6$: C, 54.38; H, 3.35; N, 12.69. Found: C, 54.33; H, 3.59; N, 12.69. Mass Spectrum (EI): m/z=331. ^{1}H-NMR ($CDCl_3$+DMSO-d_6) δ3.25 (1H, m), 4.52 (1H, m), 6.71 (1H, d),7.16 (5H, m) 8.06 (1H, dd), 8.92 (1H, d), 8.95 (1H, d).

Methyl-2-(2,4-dinitrophenylamino)-3-phenylpropanoate (4). This was prepared from 3 by the same method as in **2** (yield, ~80%) Anal. Calc. for $C_{16}H_{15}N_3O_6$: C, 55.64; H, 4.39; N, 12.17. Found: C, 56.00; H, 4.13; N, 12.04. Mass Spectrum (EI): m/z=345. ^{1}H-NMR ($CDCl_3$) δ3.33 (2H, m), 3.78 (3H, s) 4.55 (1H, m), 6.65 (1H, d), 7.27 (5H, m) 8.18 (1H, dd), 8.86 (1H, d), 9.10 (1H, d).

2-(2,4-dinitrophenylamino)-3-hydroxypropanoate (5). This was prepared from L-serine (0.518 g, 4.9 mmol) and DNFB (0.5 m*l*, 4.0 mmol) by the same method as in **1**. Yield: 0.633 g, 47%. Anal. Calc. for $C_9H_9N_3O_7$: C, 39.85; H, 3.35; N, 15.50. Found: C, 39.62; H, 3.02; N, 15.52. Mass Spectrum (EI): m/z=271. ^{1}H-NMR ($CDCl_3$+DMSO-d_6) δ3.96 (2H, m), 4.37 (1H, m), 6.87 (1H, d), 8.15 (1H, dd), 9.01 (1H, d), 9.12 (1H, d).

Methyl-2-(2,4-dinitrophenylamino)-3-hydroxypropanoate (6). This was prepared from **5** by the same method as in **2** (yield, ~85%). ^{1}H-NMR ($CDCl_3$) δ3.49 (1H, t), 3.85 (3H, s), 4.12 (2H, m), 4.45 (1H, m), 6.88 (1H, d), 8.27 (1H, dd), 9.17 (2H, d).

Ammonium 2-(2,4-dinitrophenylamino)-3-hydroxypropanoate (7). To a suspension of **5** (0.155 g, 0.6 mmol) in water (1 m*l*) was added dropwise concentrated NH_4OH until the pH of the solution became 8. After the solvent was remove by rotary evaporation the solid product was dried under vacuum and recrystallized from ethyl acetate (Yield: 0.133 g, 80%). Anal. Calc. for $C_9H_{12}N_4O_7$: C, 37.51; H, 4.10; N, 19.44. Found: C, 37.45; H, 3.69; N, 19.38. ^{1}H-NMR (D_2O) δ4.06 (2H, m), 4.38 (1H, m), 6.99 (1H, d), 8.29 (1H, dd), 9.01 (1H, d), 9.13 (1H, d).

SHG Efficiency Measurement. SHG measurements were made using the Kurtz powder method[15] with some modifications. A schematic diagram of the measurement system is shown in Figure 1. The sample cell has a thickness of 0.30± 0.05 mm. KDP (potassium dihydrogen phosphate) and urea were used as reference materials. The particle size of the reference materials was 90-100 μm. Samples were ground to a fine powder with a mortar and pestle. The particle size of the samples was estimated to 50-100 μm. No effort was made to examine the materials for phase-matchability. Errors in the measured SHG efficienceies can be quite large since the variation in grain size and the possibility of preferential orientation of particles were not taken into consideration.

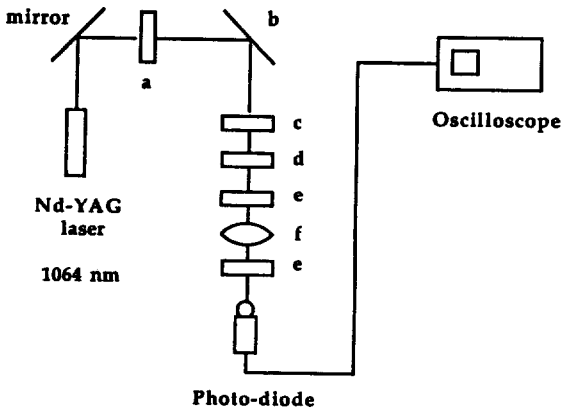

Figure 1. Schematic diagram of SHG efficiency measurement system by the powder method: (a) broad band filter, (b) harmonic beam splitter, (c) aperture, (d) sample, (e) filter, (f) lens.

Table 1. Crystallographic Data for **3**, **4** and **7**

Compound	3	4	7
formula	$C_{15}H_{13}N_3O_6$	$C_{16}H_{15}N_3O_6$	$C_9H_{12}N_4O_7$
f. w.	331.29	345.31	288.22
space group	monoclinic, $P2_1$	orthorhombic, $P2_12_12$	monoclinic, $P2_1$
a, Å	7.294(1)	12.985(5)	4.790(1)
b, Å	19.147(4)	18.400(10)	6.503(1)
c, Å	10.760(2)	13.727(6)	19.655(6)
β, deg	98.823(6)		90.88(1)
vol, Å^3	1485.0(4)	3280(3)	612.2(3)
Z	4	8	2
temp, ℃	23	23	23
d(calcd), g/cm^3	1.481	1.400	1.560
λ(MoKα$_1$), Å	0.70926	0.70926	0.70926
monochromator	graphite	graphite	graphite
linear abs. coeff., cm^{-1}	1.1	1.0	1.3
crystal size, mm	0.35×0.28 ×0.06	0.38×0.50 ×0.25	0.06×0.10 ×0.30
crystal color	yellow	yellow	yellow
θ limits, deg	50	46	50
No. of unique data	4273	2870	1197
No. of unique data with $F_O^2>3\sigma(F_O^2)$	2581	2528	719
No. of variables	444	451	180
R	0.044	0.049	0.072
R_w	0.047	0.049	0.081

X-ray Crystal Structure Determination. Crystal structures of **3**, **4** and **7** were determined by the single crystal X-ray diffraction methods. Crystals of **3** were obtained by slow diffusion of water into the methanol solution of **3** and those of **4** and **7** by slow evaporation of their methanol solutions. X-ray data were collected on an Enraf-Nonius CAD4 diffractometer using MoKα radiation at room temperature. Cell parameters and an orientation matrix for data collection were obtained from least squares refinement, using the setting angles of 25 reflections in the range of $18.0°<2\theta<28.0°$. The crystallographic data and additional details of data collection are summarized in Table 1. The intensities of 3 stan-

Table 2. Positional and Equivalent Isotropic Thermal Parameters for **3**

Atom	*x*	*y*	*z*	B_{eq}(Å^2)
01′	0.6260(6)	0.186	0.9956(4)	5.1(1)
01	0.7611(7)	0.0752(2)	0.5251(4)	5.2(1)
02′	0.4139(7)	0.2062(2)	0.8385(5)	7.3(1)
02	0.9371(7)	0.0512(2)	0.6990(4)	4.6(1)
03′	0.3194(7)	−0.0619(2)	0.5376(4)	5.4(1)
03	1.1086(7)	0.2191(2)	1.0141(4)	5.8(1)
04′	0.2163(6)	0.0433(2)	0.5235(4)	5.3(1)
04	1.0960(6)	0.3290(2)	0.9680(4)	4.9(1)
05	0.4168(5)	0.2788(2)	0.1929(4)	3.83(9)
05′	1.0338(6)	−0.0135(2)	1.2963(3)	4.1(4)
06′	0.9356(7)	0.0965(2)	1.2601(4)	5.2(1)
06	0.4621(6)	0.1677(2)	0.2583(4)	5.0(1)
N1	0.7223(6)	0.2060(2)	0.4488(4)	2.9(1)
N1′	0.7808(7)	0.0630(3)	1.0252(4)	3.6(1)
N2′	0.5242(7)	0.1672(3)	0.8993(5)	4.1(1)
N2	0.8545(7)	0.0927(3)	0.6247(4)	3.7(1)
N3	1.0637(7)	0.2676(3)	0.9397(4)	4.0(1)
N3′	0.3129(7)	−0.0028(3)	0.5778(4)	4.0(1)
C1′	0.6629(8)	0.0465(3)	0.9208(5)	2.8(1)
C1	0.8022(7)	0.2192(3)	0.5672(5)	2.8(1)
C2	0.8661(8)	0.1671(3)	0.6558(5)	2.7(1)
C2′	0.5364(8)	0.0967(3)	0.8552(5)	2.8(1)
C3′	0.4221(8)	0.0787(3)	0.7459(5)	3.0(1)
C3	0.9516(8)	0.1827(3)	0.7776(5)	2.9(1)
C4′	0.4281(8)	0.0140(3)	0.6973(5)	3.2(1)
C4	0.9696(8)	0.2507(3)	0.8138(5)	2.8(1)
C5	0.9076(8)	0.3054(3)	0.7314(5)	3.3(1)
C5′	0.5469(9)	−0.0372(3)	0.7592(5)	3.6(1)
C6	0.8252(8)	0.2894(3)	0.6115(5)	3.1(1)
C6′	0.6606(8)	−0.0204(3)	0.8671(5)	3.3(1)
C7′	0.9287(8)	0.0173(3)	1.0857(5)	3.3(1)
C7	0.6742(7)	0.2562(3)	0.3482(5)	2.7(1)
C8′	1.1039(9)	0.0294(3)	1.0247(5)	3.9(1)
C8	0.8310(8)	0.2674(3)	0.2700(5)	3.6(1)
C9	1.0067(8)	0.2909(3)	0.3526(5)	3.4(1)
C9′	1.2633(8)	−0.0185(3)	1.0723(5)	3.3(1)
C10	1.1261(8)	0.2423(3)	0.4145(6)	3.5(1)
C10′	1.2751(9)	−0.0843(3)	1.0185(6)	4.1(2)
C11	1.2799(9)	0.2629(4)	0.4999(6)	4.7(2)
C11′	1.419(1)	−0.1280(4)	1.0634(7)	5.4(2)
C12	1.316(1)	0.3326(4)	0.5180(6)	5.3(2)
C12′	1.551(1)	−0.1089(4)	1.1627(7)	6.0(2)
C13′	1.5413(9)	−0.0446(4)	1.2163(7)	5.6(2)
C13	1.201(1)	0.3821(4)	0.4560(7)	5.3(2)
C14	1.049(1)	0.3616(3)	0.3713(7)	4.7(2)
C14′	1.397(1)	0.0019(4)	1.1734(6)	4.7(2)
C15	0.5030(8)	0.2271(3)	0.2627(5)	3.3(1)
C15′	0.9654(8)	0.0394(3)	1.2230(5)	3.4(1)

$B_{eq}=(4/3)\Sigma_i\Sigma_j\beta_{ij}a_i\cdot a_j$.

Table 3. Positional and Equivalent Isotropic Thermal Parameters for **4**

Atom	*x*	*y*	*z*	B_{eq}(Å^2)
01′	0.3887(5)	0.6283(2)	0.4947(3)	6.1(1)
01	0.1197(5)	0.5003(2)	1.0202(4)	7.2(1)
02′	0.3960(4)	0.6598(2)	0.6453(4)	5.4(1)
02	0.1357(6)	0.4707(2)	0.8702(4)	7.9(2)
03′	0.3769(6)	0.4931(3)	0.9008(3)	8.8(2)
03	0.1693(4)	0.6393(3)	0.6178(3)	5.2(1)
04′	0.3766(4)	0.3784(3)	0.8745(3)	5.7(1)
04	0.1564(5)	0.7542(3)	0.6454(3)	6.4(1)
05′	0.3746(5)	0.5297(2)	0.2594(3)	6.5(1)
05	0.0976(5)	0.5933(3)	1.2526(4)	7.4(2)
06′	0.3381(6)	0.4166(3)	0.2091(3)	6.1(1)
06	0.0963(4)	0.7075(3)	1.3036(3)	5.4(1)
N1′	0.3454(5)	0.4935(3)	0.4455(3)	3.9(1)
N1	0.0743(4)	0.6349(3)	1.0669(4)	3.8(1)
N2′	0.3859(4)	0.6137(3)	0.5818(4)	4.4(1)
N2	0.1257(5)	0.5158(3)	0.9338(4)	4.9(1)
N3′	0.3747(5)	0.4409(3)	0.8464(4)	5.3(2)
N3	0.1577(4)	0.6913(3)	0.6728(4)	4.1(1)
C1′	0.3596(5)	0.4818(3)	0.5404(4)	3.4(1)
C1	0.1006(5)	0.6494(3)	0.9738(4)	3.3(1)
C2	0.1225(5)	0.5929(3)	0.9058(4)	3.2(1)
C2′	0.3739(5)	0.5380(3)	0.6107(5)	3.4(1)
C3	0.1437(5)	0.6069(3)	0.8089(4)	3.6(1)
C3′	0.3755(5)	0.5248(3)	0.7102(5)	3.5(1)
C4	0.1421(5)	0.6763(3)	0.7768(4)	3.3(1)
C4′	0.3703(5)	0.4543(3)	0.7421(4)	3.5(1)
C5	0.1244(5)	0.7346(3)	0.8394(4)	3.6(1)
C5′	0.3645(5)	0.3962(3)	0.6767(4)	3.6(1)
C6′	0.3601(5)	0.4093(3)	0.5802(4)	3.3(1)
C6	0.1037(5)	0.7210(3)	0.9339(5)	3.6(1)
C7′	0.3106(6)	0.4403(3)	0.3749(5)	4.0(2)
C7	0.0479(5)	0.6879(4)	1.1410(5)	3.8(2)
C8	−0.0668(6)	0.7019(4)	1.1478(5)	4.9(2)
C8′	0.1956(6)	0.4303(4)	0.3711(5)	5.0(2)
C9′	0.1525(5)	0.4043(3)	0.4673(5)	3.8(1)
C9	−0.1101(5)	0.7388(3)	1.0577(5)	3.8(1)
C10′	0.1205(5)	0.4518(3)	0.5402(5)	4.3(2)
C10	−0.1045(6)	0.8146(4)	1.0512(5)	4.9(2)
C11′	0.0905(6)	0.4268(4)	0.6305(5)	5.1(2)
C11	−0.1346(6)	0.8485(4)	0.9658(6)	6.3(2)
C12′	0.0902(6)	0.3531(5)	0.6490(6)	5.9(2)
C12	−0.1699(6)	0.8093(5)	0.8882(6)	6.5(2)
C13	−0.1796(6)	0.7356(5)	0.8958(5)	5.7(2)
C13′	0.1175(6)	0.3053(4)	0.5777(6)	5.4(2)
C14′	0.1475(6)	0.3290(4)	0.4867(5)	5.0(2)
C14	−0.1481(6)	0.6999(3)	0.9799(5)	4.7(2)
C15	0.0837(6)	0.6555(4)	1.2378(5)	4.9(2)
C15′	0.3462(6)	0.4687(3)	0.2755(5)	4.6(2)
C16′	0.3607(9)	0.4372(4)	0.1091(5)	7.5(3)
C16	0.1255(7)	0.6836(5)	1.4016(5)	6.7(2)

$B_{eq}=(4/3)\Sigma_i\Sigma_j\beta_{ij}a_i\cdot a_j$.

Table 4. Positional and Equivalent Isotropic Thermal Parameters for **7**

Atom	*x*	*y*	*z*	B_{eq}(Å^2)
01	0.816(2)	0.614	0.7132(4)	4.3(2)
02	1.052(3)	0.688(2)	0.8008(5)	7.8(3)
03	0.964(2)	0.331(2)	1.0110(4)	5.3(3)
04	0.602(2)	0.138(2)	1.0229(4)	4.5(2)
05	0.510(2)	−0.022(2)	0.5980(4)	3.5(2)
06	−0.069(2)	0.222(2)	0.5851(4)	3.9(2)
07	0.272(2)	0.449(2)	0.5982(4)	3.9(2)
N1	0.873(2)	0.586(2)	0.7728(5)	3.9(3)
N2	0.760(2)	0.241(2)	0.9890(5)	3.9(3)
N3	0.468(2)	0.299(2)	0.7116(5)	3.3(2)
N4	0.749(2)	0.623(2)	0.5381(5)	3.7(3)
C1	0.546(3)	0.287(2)	0.7793(6)	2.7(3)
C2	0.741(2)	0.419(2)	0.8087(6)	2.6(3)
C3	0.816(3)	0.402(2)	0.8800(6)	2.9(3)
C4	0.698(3)	0.248(2)	0.9161(5)	2.9(3)
C5	0.504(3)	0.117(3)	0.8869(6)	3.8(3)
C6	0.432(3)	0.131(2)	0.8219(6)	3.5(3)
C7	0.250(3)	0.178(2)	0.6797(6)	3.1(3)
C8	0.345(3)	−0.035(2)	0.6568(7)	4.0(3)
C9	6.148(2)	0.297(2)	0.6170(5)	2.6(2)

$B_{eq}=(4/3)\Sigma_i\Sigma_j\beta_{ij}a_i\cdot a_j$.

dard reflections, recorded every 3 h of X-ray exposure, showed no systematic changes. All the calculations were carried out with the Enraf-Nonius Structure Determination Package (SDP). The intensity data were corrected for Lorentz and polarization effects. Systematic absences suggested that **3** and **7** belong to $P2_1$ (No. 4), and **4** to $P2_12_12$ (No. 18). The structures were solved by direct methods and refined by full-matrix least-squares methods. All the nonhydrogen atoms were refined anisotropically. The positions of hydrogen atoms were idealized (d(C-H)=0.95 Å) and included in the calculations of the structure factors as fixed contributions. Each hydrogen atom was assigned an isotropic thermal parameter of 1.2 times that of attached atom. The final cycle of refinement converged to the *R* indices listed in Table 1. The atomic scattering factors were taken from International Tables[16] for the nonhydrogen atoms and from literature[17] for hydrogen. The final positional and equivalent isotropic thermal parameters of the nonhydrogen atoms for **3**, **4** and **7** are listed in Table 2, 3, and 4, respectively.

Results and Discussion

MAP and its analogues studied in this work are displayed in Figure 2. Reactions of 2,4-dinitrofluorobenzene with L-amino acids alanine, phenylalanine and serine produced **1**, **3**, and **5**, respectively. Treatment of these acids with methanol in the presence of acid yielded the corresponding methyl esters, **2** (MAP), **4**, and **6**. The ammonium salt of **5**, **7** was obtained from the reaction of **5** with ammonium hydroxide. These were characterized by ^{1}H-NMR and mass spectroscopy, and elemental analysis.

SHG efficiencies of these compounds, measured by the

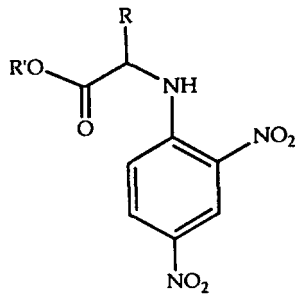

	R	R'
1	$-CH_3$	-H
2(MAP)	$-CH_3$	$-CH_3$
3	$-CH_2C_6H_5$	-H
4	$-CH_2C_6H_5$	$-CH_3$
5	$-CH_2OH$	-H
6	$-CH_2OH$	$-CH_3$
7	$-CH_2OH$	NH_4^+

Figure 2. Structures of MAP and its analogues studied in this work.

Table 5. Powder Second Harmonic Generation (SHG) Efficiencies of the MAP Analogues Relative to KDP

Compound	SHG efficiency*
KDP	1 K (1 K)
urea	5 K (3 K)
1	5 K (1.0 U)
2 (MAP)	60 K (10 U)
3	1 K
4	0.2 K
5	12.5 K (7.5 K)
6	1 K
7	17.5 K

KDP: Potassium dihydrogen phosphate. K: SHG efficiency of KDP. U: SHG efficiency of urea. *Values in parentheses are taken from ref 5, p. 221-254.

powder method[15] were listed relative to KDP (potassium dihydrogen phosphate) as standard in Table 5. As one sees in the Table 5, none of the MAP analogues exhibited SHG efficiencies as high as that of MAP. Among these, the derivatives of serine, 5 and 7 have much higher SHG efficiencies than others, but their SHG efficiencies are still ~1/5-1/4 of that of MAP. Since β values of these MAP analogues should be almost the same as that of MAP, packing of the molecules in the crystals must be responsible for the low SHG efficiencies. We therefore decided to determine the crystal structures of these MAP analogues among which we obtained crystals suitable for X-ray work for 3,4 and 7.

Crystal Structure of 3. Crystals of 3 belong to the monoclinic space group $P2_1$ with two independent molecules in the asymmetric unit. The structures of these two molecules with their relative orientations in the crystal are displayed in Figure 3. Bond distances, angles and torsional angles of the two molecules are very close to each other.[18] No bond parameters are appreciably different from the typical values in organic molecules. The amine hydrogen appears to form intramolecular hydrogen bonds with the oxygen (O1) of the neighboring nitro group (N1···O1=2.64 Å; N1'···O1'=2.62 Å) and with the oxygen (O6) of the carboxy group (N1···O6=2.68 Å; N1'···O6'=2.69 Å). The two nitro groups, amine nitrogen (N1) and the carbon atom (C7) attached to the amine nitrogen lie in the plane of the benzene ring. This suggests a good π-conjugation between the amine and the nitro groups and therefore a lage β value of the molecule.

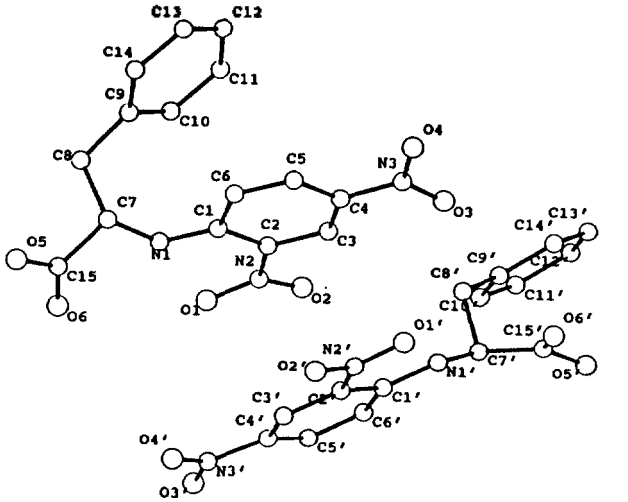

Figure 3. Structures of two crystallographically-independent molecules of 3 with their relative orientations in the crystal. Hydrogen atoms are omitted for clarity.

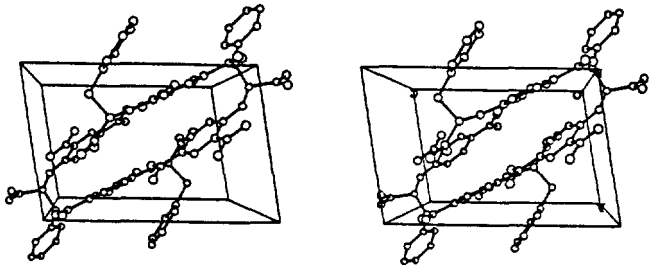

Figure 4. Stereoview of the unit cell packing of 3.

However, as discussed earlier, the SHG efficiency depends not only on the magnitude of the molecular hyperpolarizability, but also on the orientation of the molecule in the crystal lattice. Figure 4 shows the packing of molecules of 3 in the unit cell. As one sees in Figure 4 (maybe more clearly in Figure 3) the two crystallographically-independent molecules are oriented such a way that their dipoles are aligned almost antiparallel (if one considers only the dinitroaniline chromophore the structure is nearly centrosymmetric). Therefore, their contributions to bulk susceptibility $\chi^{(2)}$ cancel each other to a great extent so that the crystal of 3 does not show large second-order nonlinearity.

Crystal Structure of 4. 4 crystallizes in the orthorhombic space group $P2_12_12$ with two independent molecules in the asymmetric unit. The structures of these two molecules with their relative orientations in the crystal are shown in Figure 5 and the unit cell packing diagram in Figure 6. Bond distanes, angles and torsional angles of the two moleules

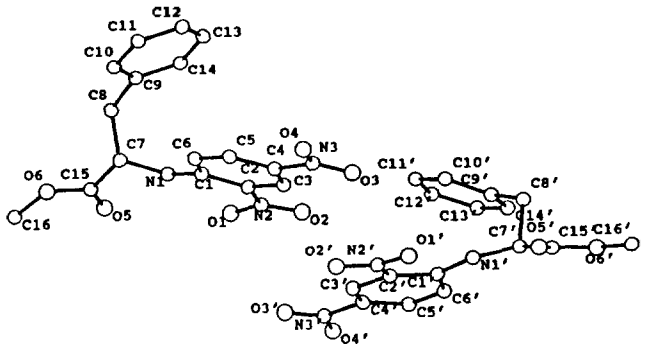

Figure 5. Structures of two crystallographically-independent molecules of **4** with their relative orientations in the crystal. Hydrogen atoms are omitted for clarity.

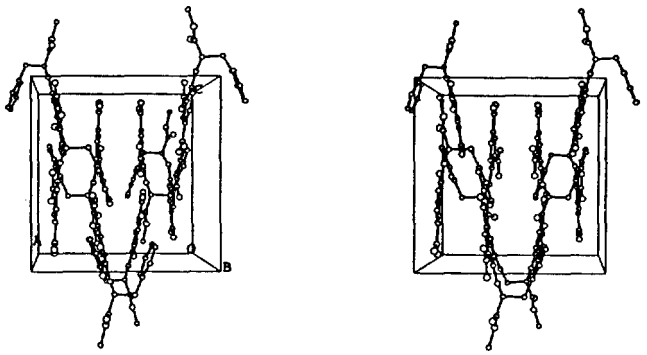

Figure 6. Stereoview of the unit cell packing of **4**.

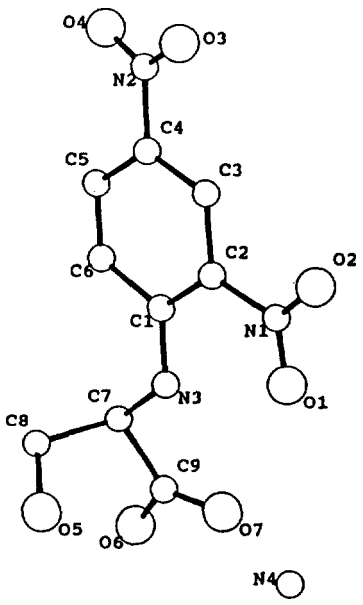

Figure 7. Sturcture of **7**. Hydrogen atoms are omitted for clarity.

are very close to each other and also to those of the corresponding acid **3** described above.[17] As in **3**, the amine hydrogen forms intramolecular hydrogen bonds with the oxygen (O1) of the nitro group and the oxygen (O5) of the carboxy group. However, most importantly, the two crystallographically independent molecules are oriented antiparallel fashion as seen in Figure 5 so that their contributions to the bulk

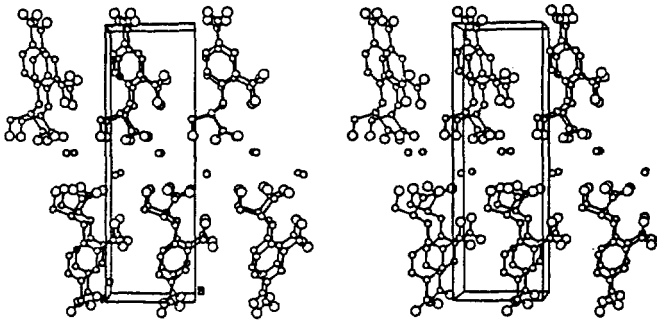

Figure 8. Stereoview of the packing of **7**.

susceptibility cancel each other to result in a very low SHG efficiency.

Crystal Structure of 7. Crystals of **7** belong to the monoclinic space group $P2_1$ with two molecules in the unit cell which are related to each other by 2_1 axis. The structure of **7** is depicted in Figure 7 and the packing of the molecules in the crystal in Figure 8. There are no unusual bond parameters found in the molecular structure of **7**.[17] One of the reasons we decided to study **5-7** was that the OH groups in these molecules would form asymmetric intermolecular hydrogen bonds which may result in higher SHG efficiencies. As expected, the OH group of **7** forms intermolecular hydrogen bonds with the carboxy group (O6') of an adjacent molecule (O5···O6' = 2.59 Å) and with the ammonium ion O5···N4 = 2.84 Å). The ammonium ion, in turn, forms another hydrogen bond with the oxygen (O7) of the nitro group. Intramolecular hydrogen bonds also exist between the amine hydrogen and the oxygens (O1 and O7) of the neighboring nitro and carboxy groups as in **3** and **4**.

In contrast to the crystal structures of **3** or **4**, that of **7** reveals substantial alignment of the dinitroaniline chromophore along the polar b axis as one sees in Figure 8. The intermolecular hydrogen bonds involving the OH group of **7** seem to contribute, at least in part, to the alignment of the dipoles. From this structure, therefore, one can easily understand the much higher SHG efficiency of **7** than those of **3** or **4**. However, the angle between the major molecular charge transfer axis (the molecular axis passing through the amino and *para*-nitro groups)[12] and the polar b axis of the crystal is approximately 86.2° that is further away from the optimum value of 54.74° for the phase-matchable SHG than that of MAP (79°). Therefore, this structure is also consistent with the lower SHG efficiency of **7** than that of MAP.

In summary, we attempted to improve the SHG efficiency of MAP by modifying the substituents on the amino group of MAP. We have prepared several MAP analogues, measured their SHG efficiencies, and determined X-ray crystal structures of some of them. The crystal structures of **3** and **4**, in which two crystallographically-independent molecules in the asymmetric unit are aligned almost antiparallel, are consistent with the very low SHG efficiencies of these compounds. On the other hand, the crystal structure of **7** reveals substantial alignment of the dinitroaniline chromophore along the polar axis. However, the angle between the molecular chage transfer axis and the polar axis of the crystal is still far away from the optimum value predicted by a theory. The structure is consistent with the SHG efficiency this co-

mpound which is much higher than 3 or 4, but still lower than that of MAP. Although the original goal has not been achieved yet, this study demonstrates the importance of the orientation of molecules in the crystal lattice in determining second-order NLO properties of crystalline materials. Further work is under way to improve the SHG efficiency of MAP by structural modifications.

Acknowledgement. This work was supported by Korea Science and Engineering Foundation and Research Institute of Industrial Science and Technology (RIST). We thank Professor Joon Won Park for helpful discussion and Mr. Dongmok Whang for the assistance in X-ray works.

References

1. P. N. Prasad and B. A. Reinhardt, *Chem. Mater.*, **2**, 660 (1990).
2. D. J. Williams, *Angew. Chem., Int. Et. Engl.*, **23**, 690 (1984).
3. P. N. Prasad and D. J. Williams, "Introduction to Nonlinear Optical Effects in Molecules and Polymers," Wiley, New York, 1990.
4. D. J. Williams, ed., "Nonlinear Optical Properties of Organic and Polymeric Materials (ACS Symposium Series 233)," American Chemical Society, Washington D. C., 1983.
5. D. S. Chemla and J. Zyss, eds., "Nonlinear Optical Properties of Organic Molecules and Crystals," Academic Press, Orlando, FL, 1987.
6. S. R. Marder, J. E. Sohn, and G. D. Stucky, eds., "Materials for Nonlinear Optics (ACS Symposium Series 455)," American Chemical Society, Washington D. C., 1991.
7. J. F. Nicoud and R. W. Twieg, in Ref. 5, Vol. 1, p. 242.
8. J. L. Oudar and R. Hierle, *J. Appl. Phys.*, **48**, 2699 (1977).
9. (a) R. W. Twieg and K. Jain, In Ref. 4, p. 57; (b) J. Zyss, J. F. Nicould, and M. Coquillay, *J. Chem. Phys.*, **81**, 4160 (1984).
10. (a) G. R. Meredith, in Ref. 4, p. 30; (b) S. R. Marder, J. W. Perry, and W. P. Schaefer, *Science*, **245**, 626 (1989).
11. M Knossow, Y. Mauguen, and C. de Rango, *Cryst. Struc. Commun.*, **5**, 723 (1976).
12. J. L. Oudar and J. Zyss, *Phys. Rev.* **A26**, 2016 (1982).
13. J. Zyss and J. L. Oudar, *Ibid.*, **A26**, 2028 (1982).
14. A more rigorous analysis[12] suggested that phase-matchable nonlinear coefficients up to 6 times larger than in MAP could be observed in compounds with similar β values but an optimum crystal structure.
15. S. K. Kurtz and T. T. Perry, *J. Appl. Phys.*, **39**, 3798 (1968).
16. International Tables for X-ray Crystallography, Vol IV., Knoch, Birmingham, England, 1974.
17. R. F. Stewart, E. R. Davison, and W. T. Simpson, *J. Chem. Phys.*, **42**, 3175 (1965).
18. Tables of bond distances, angles and torsional angles for **3**, **4** and **7** (8 pages) and anisotropic thermal parameters and observed and calculated structure factors (22 pages) are available from the corresponding author upon request.

Polymer-Supported Crown Ethers(IV) Synthesis and Phase-transfer Catalytic Activity

Jae Hu Shim*, Kwang Bo Chung, and Masao Tomoi†

Department of Chemical Engineering, Dongguk University, Seoul 100-715
†Department of Applied Chemistry, Faculty of Engineering, Yokohama National University, Yokohama 240, Japan. *Received January 3, 1991*

Immobilization method of lariat azacrown ethers, containing hydroxyl group in the side arm of crown ring, on the polymer matrix and the phase-transfer catalytic activity of thus obtained immobilized lariat azacrown ethers were studied. Polystyrene resins with crown ether structures and hydroxyl groups adjacent to the macrorings were prepared by the reaction of crosslinked polystyrene resins containing epoxy groups with monoaza-15-crown-5 or monoaza-18-crown-6. Microporous crosslinked polystyrene resins containing epoxy group for the syntheses of these immobilized lariat crown catalysts were prepared by suspension polymerization of styrene, divinylbenzene (DVB 2%) and vinylbenzyl glycidyl ether. The immobilized lariat catalysts with 10-20% ring substitution exhibited maximal activity for the halogen exchange reactions of 1-bromooctane with aqueous KI or NaI under triphase heterogeneous conditions. Immobilized catalyst exhibited higher activity than corresponding catalyst without the hydroxyl group and this result was suggested that the active site have a structure in which the K^+ ion was bound by the cooperative coordination of the crown ring donors and the hydroxyl group in the side arm.

Introduction

Polymer-supported quaternary ammonium and phosphonium ions, crown ethers, and cryptands are phase-transfer catalysts for reactions between water-soluble salts and water-insoluble organic substrates[1,2]. When the polymer is inso-